

Geohazard Detection Based on High-Precision Estimates of the Instantaneous Velocity of Autonomous GNSS Stations

Roland Hohensinn¹, Alain Geiger²

¹Institute of Geodesy and Photogrammetry, ETH Zurich, (roland.hohensinn@geod.baug.ethz.ch)

²Institute of Geodesy and Photogrammetry, ETH Zurich, (alain.geiger@geod.baug.ethz.ch)

Key words: *GNSS Instantaneous Velocity Estimation, Significance Testing, Geohazard Detection, Seismic Monitoring, Early Warning Systems*

ABSTRACT

This paper deals with the detection of small movements of a GNSS station/receiver, based on estimates of its instantaneous velocity. The accuracy of the epoch-wise velocity estimates is at a level a few millimeters per seconds; recent results also revealed that for the most precise component few tenths of mm/s are attainable. In order to detect a movement, the estimated velocity and the covariance information form the basis for the statistical tests, and the assessment of significance. An advantage of this algorithm is its real-time capability, furthermore it runs on a stand-alone GNSS station. Thus, no network connections are required, and the GNSS stations can be considered as independent and stand-alone movement detection sensor. Experimental data demonstrate that this algorithm has the potential to detect movements on the mm/s level, and below. Furthermore, we highlight its capability for the detection and localization of strong-sized earthquakes: With receiver velocity estimates for densely deployed GNSS stations, prominent seismic phases can be identified, and with a simple inversion model, the earthquake hypocenter coordinates and the source time can be estimated with remarkable quality. We conclude that the presented method might considerably contribute to a GNSS-based earthquake or landslide early warning system.

I. INTRODUCTION

High-precision estimates of instantaneous GNSS station/receiver velocity estimates can be computed based on derivatives of carrier phase measurements (Serrano et al., 2004; van Graas and Soloviev, 2004). In RINEX observation data formats, carrier phase measurements are given in units of cycles, and can be converted to delta-range measurements by multiplication with the nominal carrier frequency of the satellite signal. Differencing these carrier phase measurements yields observation quantities of Doppler shift, or observations of the velocity in receiver-to-satellite Line-of-sight (LOS), respectively. These observed velocities then consist of contributions from the radial satellite velocity, atmospheric rates, relativistic effects, receiver clock drift and receiver velocity in LOS, and several more. Typically, many of these effects are accounted by models and corrections that come with the satellite broadcast message, and beside other parameters, the receiver velocity can then be estimated epoch-wise in a least-squares adjustment, or with a recursive filter, for instance. For the obtainable accuracies of these receiver velocity estimates, values at the level of millimeters per second were reported (e.g., Ding and Wang, 2011; Wieser, 2007; Zhang et al., 2008 or Freda et al., 2015). An advantage of this method is, that -- in contrast to RTK (Real Time Kinematic) positioning or real-time PPP (Precise Point Positioning) -- no real-time corrections

from reference stations or reference networks are needed, but only the data from the individual satellites' broadcast navigation message. Therefore it can be operated in a complete standalone mode, applicable for autonomous GNSS stations. However, the estimation of instantaneous GNSS receiver velocities has not been investigated that extensively as real-time positioning algorithms. Recently, this method for obtaining high-precision velocity estimates was revised in detail, with the purpose of using it to detect hazardous ground movements with autonomous GNSS stations (Hohensinn et al., 2018; Hohensinn et al., 2019). The motivation for this work was to rapidly assess whether a GNSS station is moving or not -- such movements may be caused by landslides or earthquakes, for example. The goal is to support natural hazard early warning systems with real-time information from GNSS dynamic monitoring. Such early warning systems shall help to prevent humans and infrastructure from damage. Based on the epoch-wise estimated instantaneous receiver velocity and the covariance information of the velocity estimates, a statistical significance test can be carried out, and movements can be detected. The method is particularly suited for high-rate GNSS, with sampling rates of 1 Hertz and higher. With measurement data coming from experiments with a shake table and a robotic arm, it was shown that the presented algorithm has the potential to resolve movements on the millimeter-per-second level, and even below. In Hohensinn and Geiger,

2018 it was also demonstrated how this algorithm can be used to detect strong earthquakes based on GNSS measurements. Furthermore, a GNSS-only earthquake hypocenter localization based on the detected first arrivals of the seismic waves comes very close (less than a kilometer) to the solution provided by official seismic services.

It is also planned to run the developed algorithm on autonomous GNSS monitoring stations in the Swiss Alps. These stations are being developed by the Institute of Geodesy, as well as by project partners at ETH. Figure 1 illustrates such an autonomous monitoring station, located in the Swiss Alps. Former works of the Institute were also dedicated to the development of algorithms than can detect movements of autonomous GNSS stations in real time (Guillaume and Geiger 2007; Guillaume et al. 2012).



Figure 1: Example of a self-sufficient GNSS monitoring station, developed by the Institute of Geodesy and Photogrammetry of ETH Zurich (Image: Phillipe Limpach)

In this contribution we will give an overview of the algorithm that was developed for the detection of movements from instantaneous velocity estimates (section 2). We start with introducing the reduced velocity observation equation, and then highlight important aspects on the parameter estimation and quality control. Then the test quantity for the epoch-wise detection of movements is introduced, as well as a decision criterium, which extends over several epochs. In section 3, results are presented: On the one hand, for an experiment with a robot arm, where a slow sinusoidal movement was tested, as well as for the detection and localization of strong earthquakes, with an example of the 6.5 Mw earthquake in Central Italy of October 2016. In section 4, we summarize the most

important findings, and highlight some aspects on the improvement potential of the presented algorithm.

II. METHODOLOGY

A. GNSS Instantaneous Velocity Estimation

The velocity observations are range rates (satellite-receiver LOS velocity), obtained by time-differentiation of GNSS phase measurements, after they were converted to units of meters. Prominent effects like the LOS satellite velocity, satellite clock drift, atmospheric and relativistic effects are then accounted for by models obtained from the satellite broadcast message. The velocity observations were then reduced by these effects, which results in a reduced observation equation of the form

$$v_{r,RED}^i(t) = (\mathbf{v}_r(t))^T \mathbf{a}_r^i(t) - c\delta\dot{t}_r(t) + \dot{\epsilon}_i(t) \quad (1)$$

where $v_{r,RED}^i(t)$ is the reduced velocity observation (m/s) from receiver r to satellite i at GNSS system time t , $\mathbf{v}_r(t)$ is the receiver velocity vector (cartesian components, WGS84), $\mathbf{a}_r^i(t)$ is the receiver-satellite LOS unit vector, c is the speed of light, $\delta\dot{t}_r(t)$ is the receiver clock drift and $\dot{\epsilon}_i(t)$ is the observation error, which consists of the time derivate of GNSS phase noise, as well as remaining errors not captured by the models. The receiver-to-satellite unit vectors are obtained from a code SPP (Single Point Positioning) solution, which is accurate enough for this purpose. Together with a term for the receiver clock drift, they make up the functional model for the adjustment. For each epoch, the parameters to be estimated are the three components of the receiver velocity vector and the receiver clock drift. The solution for the unknown parameters (estimates) of the batch weighted least-squares estimator is

$$\hat{\mathbf{x}} = (\mathbf{A}^T \mathbf{Q}_y^{-1} \mathbf{A})^{-1} \mathbf{A}^T \mathbf{Q}_y^{-1} \mathbf{y} \quad (2)$$

with the covariance matrix of the parameters

$$\mathbf{Q}_{\hat{\mathbf{x}}} = (\mathbf{A}^T \mathbf{Q}_y^{-1} \mathbf{A})^{-1} \quad (3)$$

\mathbf{A} is the design matrix; the reduced velocity observations are in \mathbf{y} . The stochastic model is defined by \mathbf{Q}_y ; its main diagonal contains the variances of the velocity observations. They are determined in a calibration based on observation residuals from static phases, based on the root mean square error (RMSE) values, and are assumed to be uncorrelated.

B. Quality Control

For the quality control of the observations, the DIA (Detection-Identification-Adaption) method for weighted least-squares estimators in batch mode was implemented (e.g., Teunissen and Kleusberg, 1998; Teunissen, 2017). For each epoch, the least-squares

residuals were computed by $\hat{\mathbf{e}} = \mathbf{y} - \hat{\mathbf{y}}$, with $\hat{\mathbf{y}} = \mathbf{A}\hat{\mathbf{x}}$, and the covariance matrix $\mathbf{Q}_{\hat{\mathbf{e}}} = \mathbf{Q}_y - \mathbf{A}\mathbf{Q}_{\hat{\mathbf{x}}}\mathbf{A}^T$. For failure detection, the overall model test was then computed by $\hat{\mathbf{e}}^T \mathbf{Q}_{\hat{\mathbf{e}}}^{-1} \hat{\mathbf{e}}$, which under H_0 is assumed to be Chi-square distributed. The test quantity is compared against $\chi_{\alpha_D}^2(f, 0)$ with $f = n - 4$ degrees of freedom (n is the number of observations) at a level of significance α_D , and a non-centrality parameter of zero. If the overall model test was indicating a fault, data snooping was applied to check for single gross errors (local slippage) in the observations: For uncorrelated observations, the test quantity for the i -th observation is $\hat{e}_i / \sigma_{\hat{e}_i}$, which under H_0 is assumed to follow a standard normal distribution. The test quantity is compared against the standard normal distribution $\mathcal{N}_{\alpha_1/2}(0, 1)$, at a level of significance α_1 . Amongst i test values, the bad observation indicated by the largest test value exceeding the normal distribution criterion was then corrected for in the estimates and the covariance matrix, and the test procedure was repeated.

C. Movement Detection and Decision Making

The epoch-wise movement detection test is based on the estimated velocity vector $\hat{\mathbf{v}}$ (dimension 3×1) and the covariance matrix of the velocity estimates $\mathbf{Q}_{\hat{\mathbf{v}}}$ (dimension 3×3), respectively. For each epoch, both can be extracted from the estimated parameter vector $\hat{\mathbf{x}}$ (dimension 4×1) and the covariance matrix of the estimated parameters $\mathbf{Q}_{\hat{\mathbf{x}}}$ (dimension 4×4), respectively. The test quantity for the statistical hypothesis test on significant velocities is formulated by

$$T_{mov} = \hat{\mathbf{v}}^T \mathbf{Q}_{\hat{\mathbf{v}}}^{-1} \hat{\mathbf{v}} \quad (4)$$

This quantity is Chi-square distributed $T_{mov} \sim \chi(3, 0)$ with 3 degrees of freedom, and a non-centrality parameter of zero in the case for no velocity, and $\hat{\mathbf{v}}$ being unbiased. Based on this information, a null and an alternative hypothesis can be specified by

$$\begin{aligned} H_0: \text{no movement} \dots T_{mov} &\sim \chi(3, 0) \\ H_A: \text{movement} \dots T_{mov} &\sim \chi(3, \lambda) \end{aligned}$$

with a non-centrality parameter λ . The null hypothesis is that there is no station movement (no significant velocity), and the alternative hypothesis is that the station is moving (significant velocity). For each epoch, test quantity of eqn. (4) is compared to the limit of the Chi-square distribution $\chi_{\alpha}(3, 0)$, where α is the level of significance, a non-centrality parameter of zero, and a degree of freedom of three, since the test includes all three elements of the velocity vector. For the movement detection test, a significance level of 0.5% was chosen for the work presented here.

Beside this movement detection test, another interesting quantity to analyze is the minimum detectable velocity (MDV). It can be computed by a principal component analysis of the covariance matrix

$\mathbf{Q}_{\hat{\mathbf{v}}}$, and refers to the shortest axis of the confidence ellipsoid (for a given significance level and test power). More details can be found in Hohensinn et al., 2018.

The movement test is carried out epoch-wise with the test quantity of eqn. (4). For making a decision (does the station move or not?), a movement detection test including only a single epoch may be insufficient because of two reasons: There will be false alarms due to the chosen level of significance, and false alarms due to remaining biases in the observations (propagating into the estimates), which are not captured by the quality control procedure. Therefore, multiple epochs should be involved to reach a decision. One possibility is to extend the single epoch test criterion of eqn. (4) over multiple epochs, which then becomes $\sum_k^k \hat{\mathbf{v}}_k^T \mathbf{Q}_{\hat{\mathbf{v}}_k}^{-1} \hat{\mathbf{v}}_k$, with $3 \times k$ degrees of freedom. However, this still might be strongly affected by biases in the observations which cannot be resolved by the outlier test at a single epoch. The movement detection criterium used here is based on a cumulative relative frequency criterion. It is a rather heuristic, but effective: Over multiple epochs, the relative cumulative frequency of detections in a window with N samples is computed. Input are booleans of the epoch-wise detection result based on eqn. (4), over all N past epochs (1 for a detection and 0 otherwise):

$$P_n = \frac{1}{N} \sum_{k=0}^{N-1} b_{n-k}^{mov} \quad (5)$$

Finally, if this quantity exceeds a certain threshold, it is decided to be a movement, and a global movement flag can be set to "yes" then.

$$Movement = \begin{cases} \text{Yes} \dots & \text{if } P_n \geq \text{threshold} \\ \text{No} \dots & \text{if } P_n < \text{threshold} \end{cases}$$

Herein, this decision criterion will be used to decide if a hazardous ground movement is going on. The beginning of a movement will be referred to the first epoch, were the epoch-wise movement detection test is positive.

III. RESULTS

This section shows the results for the application of the algorithm presented in the last section for two datasets of GNSS measurements: The first one is an experiment carried out for movements with an industrial robot arm, and the second one comes from GNSS measurements of a strong earthquake in Central Italy.

A. Experiment with the Robot Arm

The capabilities of the algorithm shall be demonstrated by an experiment with a robot arm (Hohensinn et al., 2019). The test was carried out on the roof of our premises. The GNSS antenna was mounted

on the robot arm (Figure 2), and then the robot was moved with a well-defined input signal. The GNSS equipment consisted of a Septentrio PolaRx receiver and a Septentrio choke ring antenna. The sampling rate for the GNSS receiver was set to 1 Hertz. For this experiment, the input signal the robot was driven with was a 1D horizontal sinusoidal movement with a period of 100 seconds, and an amplitude of 10 centimeters. The maximum velocity of the movement was about 6 millimeters per second. About 6 full cycles of the sinusoidal movement were measured, and the duration of the measurement was about 18 minutes in total (with static phases before and after the movement). This gives about 1100 measurement epochs in total.



Figure 2: Robot arm with the GNSS antenna mounted. For the tests, the robot was moved back and forth with a 1D horizontal sinusoidal movement.

The reduced velocity observations to 9 GPS and 5 Galileo satellites were formed, at two frequencies for each GPS satellite, and three frequencies for each

Galileo satellite. The reduced observations were then averaged over the frequency bands for each satellite, for both GPS and Galileo. For each epoch there were reduced velocity observations to 14 satellites then. The set-up chosen for the quality control of the observations can be found in the appendix, together with the results for the outlier detection test (Figure 7). Figure 3 (a) shows the magnitude of the estimated receiver velocity, as well as the movements that were detected epoch-wise based on the test quantity in eqn. (4). The sinusoidal movement can be very well resolved. For the static phase right before the movement, the RMS of the velocity estimates lies between 1 and 2 mm/s. Figure (b) shows result after applying the decision criterium of eqn. (5) (with 3 out of 4 epochs). False alarms can be handled with it. For this experiment, the minimum detectable velocity was found to be at around 0.97 mm/s, and a comparison with a very precise ground truth provided by the robot underlines the feasibility of the results (Hohensinn et al. 2019).

B. Earthquake in Central Italy

The second dataset, for which the algorithm was tested with, are GNSS measurements of a strong earthquake in Central Italy (Hohensinn and Geiger, 2019). The event of interest is the 6.5 Mw earthquake near the city of Norcia, which occurred on the 30th of October, 2016. In this region, a dense network of GNSS stations is deployed (RING, 2018). Figure 4 shows a map of the GNSS stations that were processed, as well as the epicenter coordinates of the earthquake. From this network, the measurements of 42 GNSS stations were used as an input for the algorithm presented in the last section. The station distance from the epicenter ranges from few kilometers up to around 170 kilometers, and the data was processed at sampling rates of 1 Hertz and 2 Hertz, respectively. Each station was processed autonomously and in a real-time capable mode: The

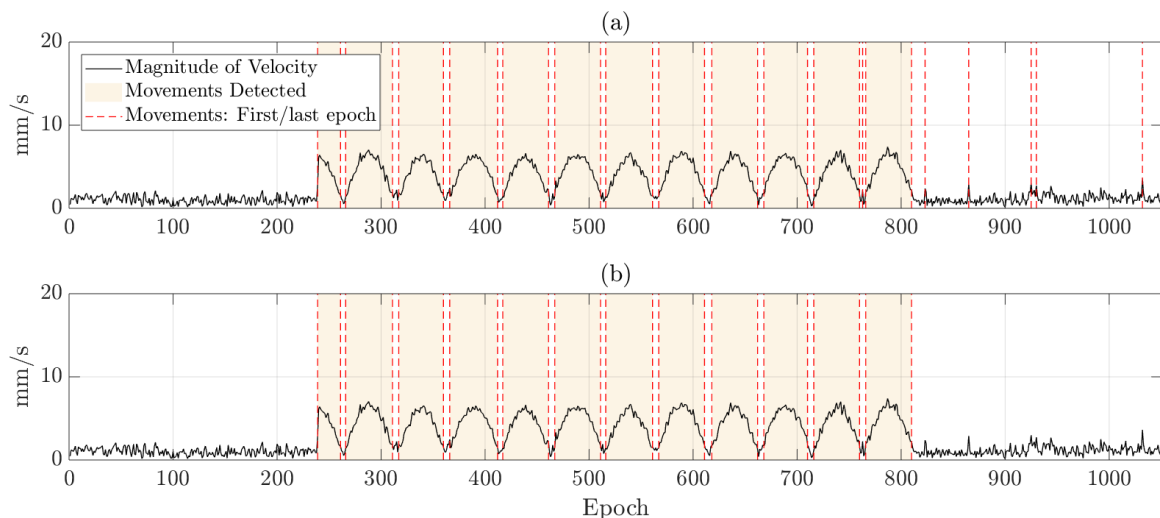


Figure 3: Plot (a) shows the magnitude of the estimated GNSS receiver velocity, and the movements that were detected epoch-wise. Plot (b) shows the detected movements after applying the cumulative decision criterium.

instantaneous velocities were estimated for each station from GPS observations, and the movement detection test was then applied for each epoch.

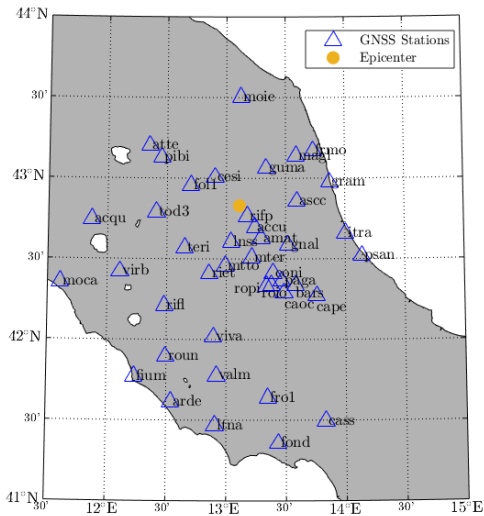


Figure 4: GNSS stations that were processed for the 6.5 Mw earthquake in Central Italy of October 30th, 2016. The yellow dot indicates the epicenter coordinates.

The decision criterium of eqn. (5) was chosen to indicate a movement if 7 out of 8 epochs of the epoch-wise test were positive. Whenever this criterium was positive, the time of the first arrival of the seismic waves were then determined by choosing the first epoch where the epoch-wise detection test was positive. The results

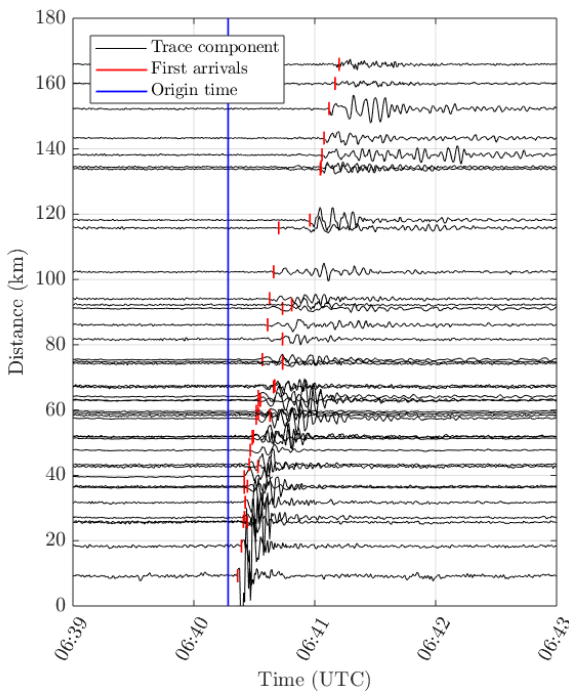


Figure 5: Seismic traces for the topocentric North component of the GNSS station velocity. Each line represents a station. The horizontal axis indicates time (UTC), and the vertical axis is the epicentral distance (km).

are presented in Figure 5 for the North topocentric station velocity component. It can be noticed that the arrivals of the seismic waves were detected in all 42 GNSS stations (vertical red bars). The arrival of seismic primary waves, up to a station distance of about 120 km, could be verified by comparison with seismometer measurements (Hohensinn and Geiger, 2019). The magnitude of the maximum station velocities range from around 1 cm/s for the furthest station, and around 5 dm/s for the station closest to the earthquake. The time-of-first arrival of the seismic waves was then used for a GNSS-only hypocenter determination of the earthquake. Based on a simple seismic velocity model, the hypocenter coordinates of the earthquake (together with the origin time) are estimated sequentially: It was started with the arrival times of an initial set of 7 stations, and then with each new detected arrival of a station, the hypocenter estimate was updated. Figure 6 shows the results for a comparison with a precise (official) reference solution, both for the East and North component, as well as for the focal depth of the earthquake (red lines). The blue band indicates the standard deviation of the hypocenter estimates.

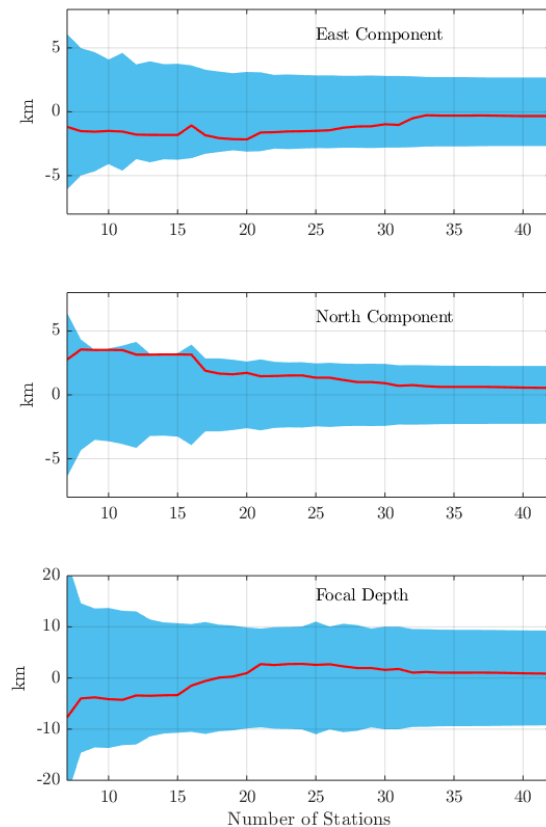


Figure 6: Results from the GNSS-only earthquake hypocenter estimation. The red lines indicate the difference w.r.t. a reference solution. The blue band indicates the standard deviation of the estimates.

The GNSS-only hypocenter localization comes as close as 1 kilometer to the reference solution. It can be concluded that GNSS with densely deployed stations can give an independent contribution to an earthquake early warning system for strong earthquakes.

IV. CONCLUSIONS

The motivation for this work was the need for a real-time algorithm to detect hazardous ground movements by means of autonomous and stand-alone GNSS stations. These stations can be situated in high-alpine regions in the Swiss alps, and the aim is to monitor and detect slope movements like landslides, or rockfalls. It was shown that this can be achieved with estimates of the instantaneous GNSS receiver velocity: Starting with time derivatives of GNSS carrier phase measurements, reduced satellite-to-receiver LOS velocity observations were formed, and the receiver velocity vector was estimated epoch-wise at rates of 1 Hz and higher. For each epoch, the estimated velocity vector can be tested for significance – and if it is found to be significant, a movement is detected. Since there can be false alarms, a decision criterium shall include multiple epochs. Movement information can be provided within seconds, and it thus can give an important contribution to natural hazard early warning systems. The algorithm was successfully tested to detect and localize a strong earthquake in Central Italy. However, there are still open issues: The integrity monitoring of the observations has to be further developed, in order to enhance the reliability of the velocity estimates, and the quality of the velocity observations could still be further investigated in terms of multi-GNSS and multi-frequency processing, for example to reduce remaining effects of the ionosphere or the wet part of the troposphere. Current research also focusses on a further development of the statistical movement detection tests.

V. ACKNOWLEDGEMENTS

This work was funded by the Swiss National Science Foundation (program *nano-tera*, project *X-Sense2*).

References

- Serrano, L., Kim, D., and Langley, R. (2004). A single GPS receiver as a real-time, accurate velocity and acceleration sensor. Proceedings of the the 17th International Technical Meeting of the Satellite Division of The Institute of Navigation (ION GNSS 2004).
- van Graas, F. and Soloviev, A. (2004). Precise velocity estimation using a stand-alone GPS receiver. *Navigation*, 51(4):283–292.
- Ding, W. and Wang, J. (2011). Precise velocity estimation with a stand-alone GPS receiver. *Journal of Navigation*, 64(2):311–325.
- Wieser, A. (2007). GPS based velocity estimation and its application to an odometer. Shaker Verlag Aachen.

- Zhang, J., Zhang, K., Grenfell, R., and Deakin, R. (2008). On real-time high precision velocity determination for standalone GPS users. *Survey Review*, 40:366–378.
- Freda, P., Angrisano, A., Gaglione, S., and Troisi, S. (2015). Time-differenced carrier phases technique for precise GNSS velocity estimation. *GPS Solutions*, 19(2):335–341.
- Guillaume, S. and Geiger, A. (2007). Real-time small movement detection with a single GPS carrier phase receiver. In Proc. European Navigation Conference, 29 – 31 May 2007, Geneva, Switzerland, pages 506–516.
- Guillaume, S., Geiger, A., and Forrer, F. (2012). G-MoDe detection of small and rapid movements by a single GPS carrier phase receiver. VII Hotine-Marussi Symposium, Rome, 6-10 June, 2009. Springer Berlin, Heidelberg.
- Teunissen, P. and Kleusberg, A. (1998). *GPS for Geodesy*. Springer-Verlag Berlin Heidelberg.
- Teunissen, P. and Montenbruck, O. (2017). *Springer handbook of Global Navigation Satellite Systems*. Springer.
- Teunissen, P. J. (2017). Batch and recursive model validation. In Teunissen and Montenbruck (2017), pages 687–720.
- Hohensinn, R. and Geiger, A. (2018). Stand-alone GNSS sensors as velocity seismometers: Real-time monitoring and earthquake detection. *Sensors*, 18(11):3712.
- Hohensinn, R., Geiger, A., and Meindl, M. (2018). Minimum detectable velocity based on GNSS Doppler phase observables. In European Navigation Conference (ENC) in Gothenburg, Sweden, 2018. IEEE.
- Hohensinn, R., Geiger, A., Willi, D., and Meindl, M. (2019). Movement detection based on high-precision estimates of instantaneous GNSS station velocity. *Journal of Surveying Engineering* (forthcoming).
- Rete Integrata Nazionale GPS (2018). High-rate GPS data archive of the 2016 Central Italy seismic sequence. <http://ring.gm.ingv.it/?p=1333>, Last accessed on 2018-08-18.

APPENDIX

For the quality control of the velocity observations, the limit for the (local) outlier test was chosen with 0.1%. The limit for the Chi-square overall model test was chosen with the b-method of testing (e.g., Teunissen and Kleusberg, 1998). Figure 7 shows the results of the Chi-square overall model test. The red spikes indicate outliers that have been identified and corrected for. In total, around 40 outliers have been corrected for.

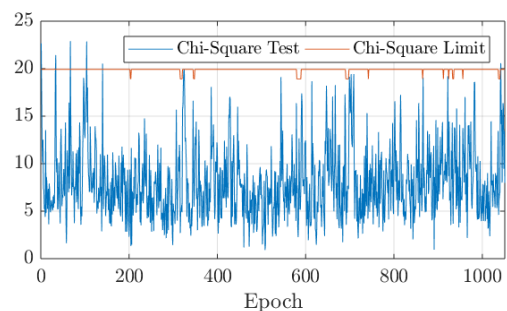


Figure 7: Results for the Chi-square overall model test of the observation quality control procedure.